

Stress-Measure Dependence of Phase Transformation Criterion under Finite Strains: Hierarchy of Crystal Lattice Instabilities for Homogeneous and Heterogeneous Transformations

Hamed Babaei¹ and Valery I. Levitas^{1,2,3}

¹*Department of Aerospace Engineering, Iowa State University, Ames, Iowa 50011, USA*

²*Departments of Mechanical Engineering, Iowa State University, Ames, Iowa 50011, USA*

³*Ames Laboratory, Division of Materials Science and Engineering, Ames, Iowa 50011, USA*

 (Received 6 November 2019; revised manuscript received 25 December 2019; accepted 17 January 2020; published 21 February 2020)

Hierarchy of crystal lattice instabilities leading to a first-order phase transformation (PT) is found, which consists of PT instability described by the order parameter and elastic instabilities under different prescribed stress measures. After PT instability and prior to the elastic instability, an unexpected continuous third-order PT was discovered, which is followed by a first-order PT after the elastic instability. Under prescribed compressive second Piola-Kirchhoff stress, PT is third order until completion; it occurs without hysteresis and dissipation, properties that are ideal for various applications. For heterogeneous perturbations and PT, first-order PT occurs when the first elastic instability criterion (among criteria corresponding to different stress measures) is met inside the volume, surprisingly independent of the stress measure prescribed at the boundary.

DOI: [10.1103/PhysRevLett.124.075701](https://doi.org/10.1103/PhysRevLett.124.075701)

Introduction.—Theoretical description of the mechanical stability of a crystal lattice is one of the essential bases for understanding structural transformation in solids. The loss of stability of crystal lattice causes structural transformations such as martensitic or displacive PTs, melting, amorphization, twinning, dislocation nucleation, cavitation, and fracture [1–7]. Therefore, crystal lattice instability criteria have fundamental importance. However, despite the numerous previous works in this direction, there are several outstanding problems to be resolved when instability occurs at finite strains.

The authors of the general elastic instability criteria for finite strains [8,9] expressed them in terms of arbitrary measures of stress and work-conjugate strain and emphasized that the instability criteria depend on the chosen (prescribed) stress or strain measure. Since for heterogeneous solutions of a boundary-value problem stress tensors can only be prescribed at the external boundary, it is impossible to define which stress measure is prescribed at each material point, i.e., elastic instability is ambiguous. For applications, practically all instability criteria are formulated in terms of the Cauchy stress [1–3,10–12] without justification. Other approaches discussed in textbooks, e.g., Ref. [13], define elastic instability based on loss of positive definiteness of some tensors of elastic moduli (generalizing Born's work [14] for finite strains) or of acoustic tensor [15] (generalizing Hadamard's work [16]). They include, in particular, conditions for loss of ellipticity of the elastostatic equations [17]. Since elastic

moduli and acoustic tensors depend on the choice of strain and stress measures, this leads to a similar ambiguity. Different criteria are collected and compared, e.g., in Refs. [9,18]. In mathematical literature on martensitic PTs [7,17], loss of stability is necessary for development of martensitic and twinned microstructure.

The alternative approach to the material instability was based on the utilization of the order parameters describing PTs in the spirit of the Landau theory [4]. The PT instability criterion for a homogeneous equilibrium phase under spontaneous variation of the order parameters was derived in Refs. [19,20] using a phase-field approach (PFA) to the first-order PTs under large strains and applied stress tensor. This criterion is linear in the normal components of the Cauchy stress tensor, which is confirmed by atomistic simulations for PTs Si I \leftrightarrow Si II [10–12] and graphite-diamond [21].

In this Letter we resolve some outstanding problems in the crystal lattice instability. Initially, we consider homogeneous perturbations and the PT process under a prescribed homogeneous stress measure. As it was mathematically proven in Refs. [19,20], the PT instability criteria are independent of the stress measures. We found here that they occur at the same strain. This is not the case for elastic instability. That is why one has a hierarchy of lattice instabilities corresponding to PT instability and elastic instabilities under various prescribed stress measures. When under the prescribed stress measure, the PT instability occurs prior to the elastic instability; a new type

of PT was discovered. There is no jump in strain and order parameter, which occurs for first-order PT. The equilibrium values of the order parameter, corresponding to stable elastic equilibrium, continuously vary with varying stresses, until elastic instability is reached. This PT is third order in this stress range (see Supplemental Material [22]), with the equilibrium structure Si_{in} corresponding to the intermediate structure along the initial part of the original transformation path for the first-order PT. When elastic instability is reached, the first-order PT $\text{Si}_{\text{in}} \leftrightarrow \text{Si II}$ occurs. Since the second Piola-Kirchhoff stress (PK2S)-strain curve under compression does not possess an elastic instability point, PT under the prescribed PK2S is a third-order PT until completion, and occurs without hysteresis and dissipation under cyclic loading, properties that are ideal for various applications. This opens the possibility of controlling PT order and properties by controlling prescribed stress measures.

For heterogeneous perturbations and the PT process, stresses are prescribed at the boundaries only. After satisfying the PT instability criterion and continuous third-order PT, first-order PT to the product phase occurs when the first elastic instability criterion (among criteria corresponding to different stress measures) is met inside the volume, independent of the prescribed stress measure at the boundary.

We designate contractions of tensors \mathbf{A} and \mathbf{B} over one and two indices as $\mathbf{A} \cdot \mathbf{B} = \{A_{ij}B_{jk}\}$ and $\mathbf{A}:\mathbf{B} = A_{ij}B_{ji}$; \mathbf{I} is the unit tensor; the transpose of \mathbf{A} is \mathbf{A}^T and the inverse of \mathbf{A} is \mathbf{A}^{-1} . The deformation gradient $\mathbf{F} = \mathbf{F}_e \cdot \mathbf{U}_t(\eta)$, the mapping crystal from an undeformed into a deformed configuration, is multiplicatively decomposed into elastic \mathbf{F}_e and transformational \mathbf{U}_t parts; \mathbf{U}_t maps the stress-free crystal cell of the parent phase to that of the transforming phase; η is the order parameter which varies from 0 for the parent phase to 1 for the product phase. Lagrangian strain is $\mathbf{E} = 0.5(\mathbf{F}^T \cdot \mathbf{F} - \mathbf{I})$.

Phase transformation instability.—Instability of the homogeneous equilibrium state of a phase under homogeneous perturbations can only be analyzed when a particular stress measure is prescribed at the boundary. It does not mean that the Cauchy (true) stress $\boldsymbol{\sigma}$ or the first Piola-Kirchhoff stress (PK1S) $\mathbf{P} = \mathbf{J}\boldsymbol{\sigma} \cdot \mathbf{F}^{-1T}$ (force per unit undeformed area), which directly participate in the boundary conditions, can only be prescribed; here $\mathbf{J} = \det \mathbf{F}$. Any other stress measure can be prescribed with the proper feedback and control of $\boldsymbol{\sigma}$ or \mathbf{P} in the experiment or atomistic simulations [22]. We will also use the Kirchhoff stress $\boldsymbol{\tau} = \mathbf{J}\boldsymbol{\sigma}$ and the PK2S $\mathbf{T} = \mathbf{F}^{-1} \cdot \mathbf{P} = \mathbf{J}\mathbf{F}^{-1} \cdot \boldsymbol{\sigma} \cdot \mathbf{F}^{-1T}$. We will start with prescribed \mathbf{P} .

PT instability for the thermodynamic equilibrium value $\eta = 0$ occurs and PT starts when the driving force X for change in η in the Ginzburg-Landau equation (see Ref. [22]) is getting positive and η grows. The general PT criterion that follows from this definition is derived in Ref. [20]. For cubic-to-tetragonal PT under action of three

normal-to-cubic-faces Cauchy stresses σ_i , this criterion is simplified to

$$(\sigma_1 + \sigma_2)\varepsilon_{i1}a_{e1} + \sigma_3\varepsilon_{i3}a_{e3} \geq (A + 3\Delta\psi^\theta)/J_e, \quad (1)$$

where ε_{ii} are components of the transformation strain $\varepsilon_t = \mathbf{U}_t(1) - \mathbf{I}$, $J_e = \det \mathbf{F}_e$, and a_e , A , and $\Delta\psi^\theta$ are interpolation constants in expression for $\mathbf{U}_t(\eta)$, the magnitude of the double-well barrier, and jump in the thermal energy, respectively. This instability criterion was calibrated and verified for Si I \leftrightarrow Si II PTs [23] using results of atomistic simulations [11,12].

Elastic instability is defined based on practical methods used in experiments or simulations. If for the equilibrium state under chosen fixed prescribed stresses at the boundary for some spontaneous perturbations of the deformation gradient $\Delta\mathbf{F}$ the mechanical equilibrium cannot be kept, then such a state is unstable. For homogenous states and perturbation, such an instability criterion results in the criterion presented in Ref. [8]. It is demonstrated that elastic instability conditions depend on the prescribed stress (and work-conjugate strain) measure [8,9]. We study the relationship between PT and elastic instability conditions for different prescribed stresses using PT between semiconducting Si I and metallic Si II using the PFA presented in Refs. [20,22,23]. To model homogeneous processes, we consider the solution for a single cubic finite element. Elastic energy is $\psi_e = 0.5\mathbf{E}_e:\mathbf{C}(\eta):\mathbf{E}_e$, where \mathbf{C} is the fourth-order elastic moduli tensor, which leads to linear relationship $\mathbf{T} = \mathbf{C}(\eta):\mathbf{E}_e$. Other stress measures are nonlinearly related to \mathbf{E}_e . To initiate PT, an initial value $\eta = 0.01$ is prescribed, and η cannot evolve below 0.01. We apply $\sigma_1 = \sigma_2 = 1$ GPa and perform slow strain-controlled compressive loading in the third direction, meaning that for each strain η reaches stationary value. Stress—strain E_3 curves are shown in Fig. 1 for four stress measures. They are the primary information for the analysis of instability for heterogeneous processes as well as for the case of stress-controlled loading. The strain-controlled homogeneous loading does not allow the instability to occur spontaneously.

For all stress measures, PT instability occurs at the same strain (Fig. 1). This explains how PT instability is independent of the prescribed stress measure.

For small strains, analytical expression for the equilibrium stress-order parameter (obtained from condition $X = 0$ for η varying from 0 to 1) and the corresponding stress-strain curve describe reducing stress during PT [31]. That is why when PT starts at fixed stress, it continues to complete until stress is equilibrated at the elastic branch of the product phase. In contrast, for finite strain in Fig. 1 after PT instability, each stress measure continues to grow and reaches maximum (except \mathbf{T}) corresponding to elastic instability at corresponding prescribed stress and different strains for different stress measures. Indeed, at prescribed

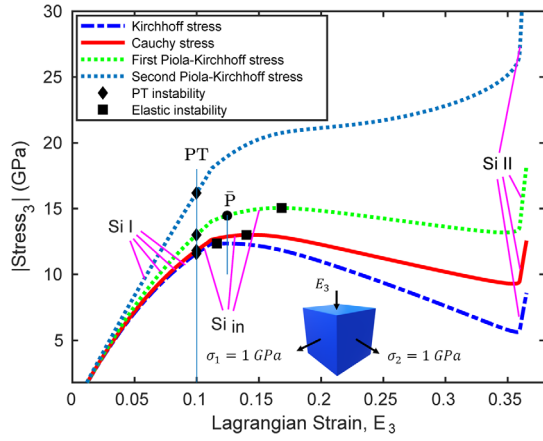


FIG. 1. Equilibrium stress-strain curves for homogeneous deformation of Si in the third spacial direction in which a strain-controlled compressive loading is applied at $\sigma_1 = \sigma_2 = 1$ GPa. Hierarchy of PT and elastic instability points are shown by markers. The intermediate phase of Si between points of PT and elastic instability, which appears via third-order PT, is designated as Si_{in}. \bar{P} is the prescribed stress for problems described below.

stress corresponding to the maximum point positive perturbation ΔE_3 leads to reduction in elastic resistance and unstable deformation transformation until PT completion and equilibration of prescribed stress at the elastic branch of the product phase. This is further analyzed considering stress-order parameter curves under three different prescribed stress measures (Fig. 2). The order parameter starts growing at stresses corresponding to PT instability in Fig. 1. With increasing stresses, the order parameter evolves in a stable equilibrium and continuous way, describing smooth transition to intermediate structures Si_{in} along the pathway Si I \rightarrow Si II. Since at PT instability stresses there is no jump in the order parameter and the corresponding jump in strain and entropy, PT initially

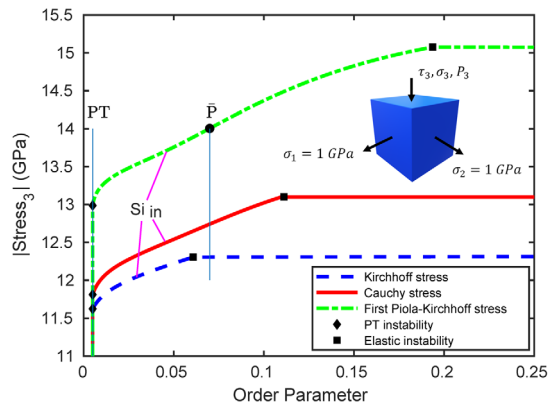


FIG. 2. Stress-order parameter curves for homogeneous deformation in the third direction in which a stress-controlled compressive loading for three different prescribed stress measures is applied at $\sigma_1 = \sigma_2 = 1$ GPa.

occurs as a third-order PT [22]. When elastic instability stress is reached for the prescribed stress measure, the order parameter grows in a nonequilibrium way to 1 and the PT proceeds until completion. This process is accompanied by a jump in the order parameter, strain, and entropy. Therefore, Si_{in} \rightarrow Si II PT is the first-order after elastic instability. Thus, a hierarchy of the PT and elastic instability points is found under different prescribed stress measures.

For the reverse, PT elastic instability and PT instability coincide and occur at the same strain $E_3 = 0.36$ corresponding to the local stress minimum for any prescribed stress measure. The difference between stresses related to elastic instability for direct and reverse PTs constitutes stress hysteresis and energy dissipation during PT. During equilibrium, third-order PT between the PT instability point and the elastic instability point, the PT or deformation is fully reversible without hysteresis for any prescribed stress. Since the equilibrium PK2S-strain curve in Fig. 1 does not have a maximum related to elastic instability point, PT under the prescribed increasing PK2S is a third-order PT until completion and occurs without hysteresis and dissipation. Reducing hysteresis and dissipation are important for various applications, e.g., for shape memory alloys [32–34] or caloric materials [34–36]; see also Ref. [10].

PT and elastic instabilities under heterogeneous perturbations in a finite volume.—During the solution of boundary-value problems with heterogeneous fields, chosen stress measure can only be prescribed at the boundary, not for each material point within the bulk. This does not allow one to directly apply elastic instability criteria obtained for homogenous states. Consequently, PT conditions under heterogeneous perturbations are not currently defined. To address this question, let us consider a PT in a sample of sizes $20 \times 60 \times 5$ nm³ under the same loading as for the homogeneous field (Fig. 3). The left face, bottom face, and one of the faces in the thickness direction are fixed by zero normal-to-the-face displacement and are symmetry planes. The right face and the other face in the

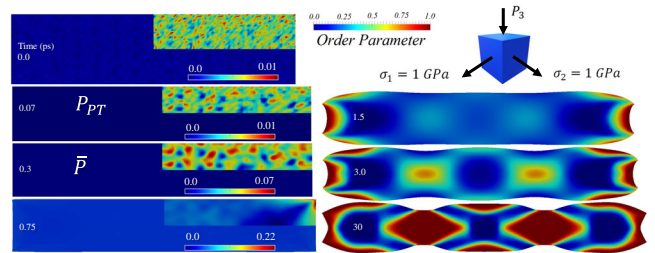


FIG. 3. Nanostructure evolution for a triaxial compressive-tensile loading with initial random heterogeneous field η in the range (0;0.01). Compressive PK1S is applied at the top face up to the value \bar{P} slightly above the peak for the Kirchhoff stress, but below the peak points for the Cauchy stress and PK1S in Fig. 1, along with $\sigma_1 = \sigma_2 = 1$ GPa. Presented solution is for the entire sample after mirroring with respect to the symmetry planes of the simulation field.

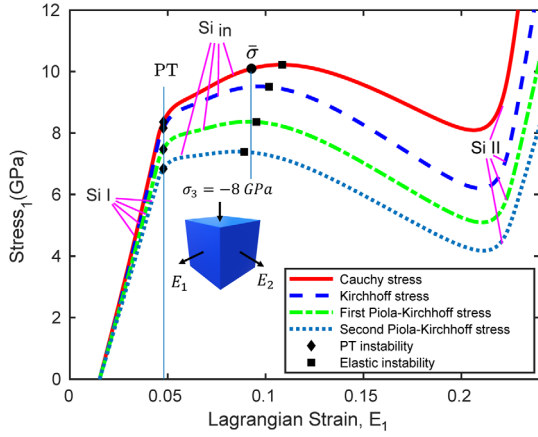


FIG. 4. Equilibrium stress-strain curves for homogeneous deformation under $\sigma_3 = -8$ GPa and increasing tensile strains $E_1 = E_2$.

thickness direction are under 1 GPa tensile Cauchy stress. The PK1S is prescribed at the top face up to a value \bar{P} slightly above the first peak point for the Kirchhoff stress, but below the peak points for the Cauchy stress and PK1S in Fig. 1. Weak heterogeneity is introduced by a random distribution of the initial values of $\eta \subseteq (0, 0.01]$. The solution is shown in Fig. 3.

From the results for a homogeneous field discussed above, we expect that for the prescribed PK1S, the PT should not continue unless we reach the PK1S peak point. Surprisingly, although the PK1S peak point is not reached yet, the exceeding strain for elastic instability for the Kirchhoff stress is sufficient for the initiation and completion of the first-order PT. Within the bulk close to the upper right corner, where the internal stresses due to heterogeneity are maximum, the critical condition for initiation of the first-order PT for the prescribed Kirchhoff stress is met locally and the region of the complete product phase is formed and grows, producing complex stationary nanostructure with significant amount of Si II. Residual austenite is stabilized by changes in geometry of the sample.

However, for different loadings, while the general principle is the same, the different stress measure produces elastic instability prior to other stress measures. For instance, we apply $\sigma_3 = -8$ GPa and increase tensile strains $E_1 = E_2$. The tensile stress-strain E_2 curves are shown in Fig. 4. In contrast to the previous compressive loading, here the PK2S peaks first and PK1S, Kirchhoff, and Cauchy stresses peak afterward. This means that PK2S should be the first elastic instability point for tensile loading under heterogeneous perturbations. For the initial values of $\eta \subseteq (0, 0.01]$ we apply $\sigma_3 = -8$ GPa and increase tensile $\sigma_1 = \sigma_2$ up to $\bar{\sigma} = 10$ GPa, slightly above the peak strain for the PK2S but lower than the peak strains for other stresses. As shown in Fig. 5, this is sufficient for initiation of the first-order PT and its completion in the major part of

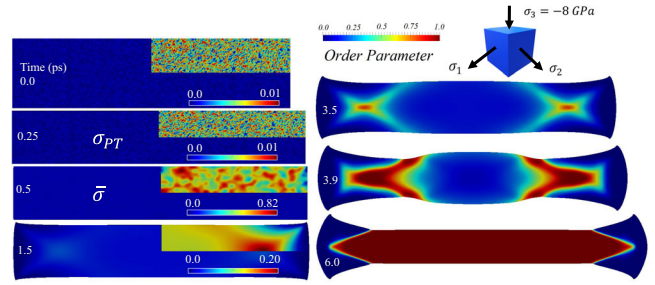


FIG. 5. Nanostructure evolution for random distribution of initial $\eta \subseteq (0, 0.01]$, $\sigma_3 = -8$ GPa and increasing tensile $\sigma_1 = \sigma_2$ up to $\bar{\sigma} = 10$ GPa, slightly above the peak strain for the PK2S but lower than the peak strains for other stresses.

the sample. Since the general expressions for the instability criteria in Refs. [8,9] are expressed in arbitrary work-conjugate stress and strain measures, one should just substitute stress measures responsible for instability obtained above for different loadings to derive specific elastic instability criteria.

In the above treatment we neglected phonon instability, which may occur before elastic instability and limit maximum stress [37–42]. In particular for Si, phonon instability occurs at hydrostatic pressure at 26 GPa [43] (well below elastic instability pressure of 75.8 GPa [12]) and at a shear strain of 0.22 for simple shear causing second-order PT [38]. These results do not affect our solutions in Fig. 1 because for uniaxial compression at $\sigma_1 = \sigma_2 = 0$ GPa phonon instability was not found before elastic instability [44]; we are not aware of any published results on phonon instability for loading considered in Fig. 4. Generally, if stress-strain curves include information about phonon instability (and other instabilities, like electronic, etc.) and the following equilibrium processes obtained with atomistic simulations (see, e.g., Refs. [24,38]), our approach can be applied in the same way. In particular, it can be applied to the PFA to PT when an order parameter describes phonon instability [45].

Conclusions.—A number of basic long-term problems in lattice instability under finite strains are resolved in this Letter. Using PFA simulations for the Si I \leftrightarrow Si II PTs, it is shown that the PT instability is independent of the prescribed stress measures because it occurs at the same strain for any prescribed stress. Prior to elastic instability and after PT instability, a continuous third-order PT is discovered, which is followed by a first-order PT after elastic instability until PT completion. Thus the transformation path changes to Si I \rightarrow Si_{in} \rightarrow Si II. Third-order PTs are quite rarely discussed in literature (see, e.g., Ref. [46] and references); we are not aware of any previous reports for elastic materials or in connection with the first-order PTs. Under prescribed compressive second Piola-Kirchhoff stress, PT is third order until completion; it occurs without hysteresis and dissipation under cyclic loading, properties that are ideal for various applications.

Since for heterogeneous perturbations stress tensors can only be prescribed at the external boundary, it is impossible to define which stress measure is prescribed at each material point, i.e., elastic instability is ambiguous. After third-order PT, the first-order PT occurs when the first elastic instability criterion (among criteria corresponding to different stress measures) is met inside the volume, surprisingly independent of the stress measure prescribed at the boundary. For two considered loadings, the elastic instability corresponds to the prescribed Kirchhoff stress and PK2S, respectively, even when the Cauchy stress was prescribed. None of our results suggests Cauchy-stress-based criterion, in contrast to most of the previous publications. This also means that finding the PT criterion from atomistic simulations [3,10–12] in terms of the Cauchy stress should be reconsidered. The general lattice instability criterion should be found for all possible prescribed stress tensors, which involves the choice of the local prescribed stresses corresponding to the first instability being different for different stress states. One more problem that was not considered here is taking into account the finite particle and lattice rotations. This problem was solved for PT instability and homogeneous perturbations in Refs. [19,20], which may help, along with the numerical procedure presented here, to treat elastic instabilities under heterogeneous perturbations.

The support of NSF (CMMI-1536925 and MMN-1904830), ARO (W911NF-17-1-0225), and Iowa State University (Vance Coffman Faculty Chair Professorship) are gratefully acknowledged. The simulations were performed at the Extreme Science and Engineering Discovery Environment (XSEDE), allocation TG-MSS170015.

[1] F. Milstein and R. Hill, Divergences among the Born and Classical Stability Criteria for Cubic Crystals under Hydrostatic Loading, *Phys. Rev. Lett.* **43**, 1411 (1979).
 [2] F. Milstein, J. Marschall, and H.E. Fang, Theoretical bcc \leftrightarrow fcc Transitions in Metals via Bifurcations under Uniaxial Load, *Phys. Rev. Lett.* **74**, 2977 (1995).
 [3] J. Wang, J. Li, S. Yip, S. Phillpot, and D. Wolf, Mechanical instabilities of homogeneous crystals, *Phys. Rev. B* **52**, 12627 (1995).
 [4] L.D. Landau and E.M. Lifshits, *Statistical Physics* (Pergamon, New York, 1980), Vol. 5.
 [5] H. Hang-Sheng and R. Abeyaratne, Cavitation in elastic and elastic-plastic solids, *J. Mech. Phys. Solids* **40**, 571 (1992).
 [6] J.M. Ball, Discontinuous equilibrium solutions and cavitation in nonlinear elasticity, *Phil. Trans. R. Soc. A* **306**, 557 (1982).
 [7] R.D. James, Finite deformation by mechanical twinning, *Arch. Ration. Mech. Anal.* **77**, 143 (1981).
 [8] R. Hill, On the elasticity and stability of perfect crystals at finite strain, in *Mathematical Proceedings of the Cambridge*

Philosophical Society (Cambridge University Press, Cambridge, England, 1975), Vol. 77, pp. 225–240.
 [9] R. Hill and F. Milstein, Principles of stability analysis of ideal crystals, *Phys. Rev. B* **15**, 3087 (1977).
 [10] V.I. Levitas, H. Chen, and L. Xiong, Triaxial-Stress-Induced Homogeneous Hysteresis-Free First-Order Phase Transformations with Stable Intermediate Phases, *Phys. Rev. Lett.* **118**, 025701 (2017).
 [11] V.I. Levitas, H. Chen, and L. Xiong, Lattice instability during phase transformations under multiaxial stress: modified transformation work criterion, *Phys. Rev. B* **96**, 054118 (2017).
 [12] N. A. Zarkevich, H. Chen, V. I. Levitas, and D. D. Johnson, Lattice Instability during Solid-Solid Structural Transformations under a General Applied Stress Tensor: Example of Si I \rightarrow Si II with Metallization, *Phys. Rev. Lett.* **121**, 165701 (2018).
 [13] A. I. Lurie, *Non-Linear Theory of Elasticity* (Elsevier, New York, 1990), Vol. 36.
 [14] M. Born, On the stability of crystal lattices. I, in *Mathematical Proceedings of the Cambridge Philosophical Society* (Cambridge University Press, 1940), Vol. 36, pp. 160–172.
 [15] R. Abeyaratne and J.K. Knowles, On the stability of thermoelastic materials, *J. Elast.* **53**, 199 (1998).
 [16] J. Hadamard, *Leçons sur la Propagation des Ondes et les Équations de l'Hydrodynamique* (A. Hermann, 1903).
 [17] J. K. Knowles and E. Sternberg, On the failure of ellipticity and the emergence of discontinuous deformation gradients in plane finite elastostatics, *J. Elast.* **8**, 329 (1978).
 [18] J. Clayton, Towards a nonlinear elastic representation of finite compression and instability of boron carbide ceramic, *Philos. Mag.* **92**, 2860 (2012).
 [19] V. I. Levitas, Phase-field theory for martensitic phase transformations at large strains, *Int. J. Plast.* **49**, 85 (2013).
 [20] V. I. Levitas, Phase field approach for stress- and temperature-induced phase transformations that satisfies lattice instability conditions. Part I. General theory, *Int. J. Plast.* **106**, 164 (2018).
 [21] Y. Peng and L. Xiong, Atomistic computational analysis of the loading orientation-dependent phase transformation in graphite under compression, *JOM* **71**, 3892 (2019).
 [22] See Supplemental Material at <http://link.aps.org/supplemental/10.1103/PhysRevLett.124.075701> for the system of equations for the phase field approach to phase transformations in elastic materials, proof of the third-order phase transformation at the phase transformation instability point before an elastic instability, and a heterogeneous field of internal stresses under triaxial compression, which includes Refs. [8–11,13,20,23–30].
 [23] H. Babaei and V. I. Levitas, Phase-field approach for stress- and temperature-induced phase transformations that satisfies lattice instability conditions. Part II. simulations of phase transformations Si I \leftrightarrow Si II, *Int. J. Plast.* **107**, 223 (2018).
 [24] R. S. Elliott, N. Triantafyllidis, and J. A. Shaw, Reversible stress-induced martensitic phase transformations in a bi-atomic crystal, *J. Mech. Phys. Solids* **59**, 216 (2011).
 [25] S. G. Lekhnitskii, *Theory of Elasticity of an Anisotropic Elastic Body* (1963).

- [26] R. G. Hennig, A. Wadehra, K. P. Driver, W. D. Parker, C. J. Umrigar, and J. W. Wilkins, Phase transformation in Si from semiconducting diamond to metallic β -Sn phase in QMC and DFT under hydrostatic and anisotropic stress, *Phys. Rev. B* **82**, 014101 (2010).
- [27] V. I. Levitas, D. L. Preston, and D.-W. Lee, Three-dimensional Landau theory for multivariant stress-induced martensitic phase transformations. III. Alternative potentials, critical nuclei, kink solutions, and dislocation theory, *Phys. Rev. B* **68**, 134201 (2010).
- [28] H. Babaei, A. Basak, and V. I. Levitas, Algorithmic aspects and finite element solutions for advanced phase field approach to martensitic phase transformation under large strains, *Comput. Mech.* **64**, 1177 (2019).
- [29] M. Parrinello and A. Rahman, Polymorphic transitions in single crystals: A new molecular dynamics method, *J. Appl. Phys.* **52**, 7182 (1981).
- [30] R. E. Miller, E. B. Tadmor, J. S. Gibson, N. Bernstein, and F. Pavia, Molecular dynamics at constant Cauchy stress, *J. Chem. Phys.* **144**, 184107 (2016).
- [31] V. I. Levitas and D. L. Preston, Three-dimensional Landau theory for multivariant stress-induced martensitic phase transformations. I. austenite \leftrightarrow martensite, *Phys. Rev. B* **66**, 134206 (2002).
- [32] J. Cui, Y. S. Chu, O. O. Famodu, Y. Furuya, J. Hattrick-Simpers, R. D. James, A. Ludwig, S. Thienhaus, M. Wuttig, Z. Zhang *et al.*, Combinatorial search of thermoelastic shape-memory alloys with extremely small hysteresis width, *Nat. Mater.* **5**, 286 (2006).
- [33] C. Chluba, W. Ge, R. L. de Miranda, J. Strobel, L. Kienle, E. Quandt, and M. Wuttig, Ultralow-fatigue shape memory alloy films, *Science* **348**, 1004 (2015).
- [34] Y. Song, X. Chen, V. Dabade, T. W. Shield, and R. D. James, Enhanced reversibility and unusual microstructure of a phase-transforming material, *Nature (London)* **502**, 85 (2013).
- [35] I. Takeuchi and K. Sandeman, Solid-state cooling with caloric materials, *Phys. Today* **68**, No. 12, 48 (2015).
- [36] H. Hou, E. Simsek, T. Ma, N. S. Johnson, S. Qian, C. Cisse, D. Stasak, N. A. Hasan, L. Zhou, Y. Hwang, R. Radermacher, V. I. Levitas, M. J. Kramer, M. Asle Zaeem, A. P. Stebner, R. T. Ott, J. Cui, and I. Takeuchi, Fatigue-resistant high-performance elastocaloric materials via additive manufacturing, *Science* **366**, 1116 (2019).
- [37] D. M. Clatterbuck, C. R. Krenn, M. L. Cohen, and J. L. Morris, Jr., Phonon Instabilities and the Ideal Strength of Aluminum, *Phys. Rev. Lett.* **91**, 135501 (2003).
- [38] S. M. M. Dubois, G. M. Rignanese, T. Pardoen, and J. C. Charlier, Ideal strength of silicon: An *ab initio* study, *Phys. Rev. B* **74**, 235203 (2006).
- [39] P. Řehák, M. Černý, and M. Šob, Mechanical stability of ni and ir under hydrostatic and uniaxial loading, *Model. Simul. Mater. Sci. Eng.* **23**, 055010 (2015).
- [40] M. Černý, P. Řehák, and J. Pokluda, The origin of lattice instability in bcc tungsten under triaxial loading, *Philos. Mag.* **97**, 2971 (2017).
- [41] M. Friák, D. Holec, and M. Šob, An *ab initio* study of mechanical and dynamical stability of mosi2, *J. Alloys Compd.* **746**, 720 (2018).
- [42] J.-H. Wang, Y. Lu, X.-L. Zhang, and X.-h. Shao, The elastic behaviors and theoretical tensile strength of γ -tial alloy from the first principles calculations, *Intermetallics* **101**, 1 (2018).
- [43] K. Gaál-Nagy and D. Strauch, Phonons in the β -tin, i m m a, and sh phases of silicon from *ab initio* calculations, *Phys. Rev. B* **73**, 014117 (2006).
- [44] N. A. Zarkevich, V. I. Levitas, H. Chen, and D. D. Johnson, Phonon spectra and instabilities in Si I and II under triaxial loadings (to be published).
- [45] P. Toledano and V. Dmitriev, *Reconstructive Phase Transitions: In Crystals and Quasicrystals* (World Scientific, Singapore, 1996).
- [46] F. D. Cunden, P. Facchi, M. Ligabò, and P. Vivo, Universality of the third-order phase transition in the constrained coulomb gas, *J. Stat. Mech.* (2017) 053303.